Journal of Visualized Experiments

Endovascular perforation model for subarachnoid hemorrhage combined with Magnetic Resonance Imaging (MRI)

--Manuscript Draft--

Article Type:	Invited Methods Collection - JoVE Produced Video
Manuscript Number:	JoVE63150R2
Full Title:	Endovascular perforation model for subarachnoid hemorrhage combined with Magnetic Resonance Imaging (MRI)
Corresponding Author:	Ran Xu, MD Charité Universitätsmedizin Berlin Campus Charite Mitte: Charite Universitatsmedizin Berlin Berlin, Berlin GERMANY
Corresponding Author's Institution:	Charité Universitätsmedizin Berlin Campus Charite Mitte: Charite Universitatsmedizin Berlin
Corresponding Author E-Mail:	ran.xu@charite.de
Order of Authors:	Shuheng Liu
	Katharina Tielking
	Dario von Wedel
	Melina Nieminen-Kelhä
	Susanne Mueller
	Philipp Boehm-Sturm
	Peter Prof. Vajkoczy
	Ran Xu
Additional Information:	
Question	**Response**
Please specify the section of the submitted manuscript.	Neuroscience
Please indicate whether this article will be Standard Access or Open Access.	Standard Access ($1400)
Please indicate the **city, state/province, and country** where this article will be **filmed**. Please do not use abbreviations.	Berlin, Germany
Please confirm that you have read and agree to the terms and conditions of the author license agreement that applies below:	I agree to the Author License Agreement
Please provide any comments to the journal here.	
Please confirm that you have read and agree to the terms and conditions of the video release that applies below:	I agree to the Video Release

TITLE:

Endovascular Perforation Model for Subarachnoid Hemorrhage Combined with Magnetic Resonance Imaging (MRI)

AUTHORS AND AFFILIATIONS:

Shuheng Liu[1*], Katharina Tielking[1*], Dario von Wedel[1], Melina Nieminen-Kelhä[1], Susanne Mueller[2,3], Philipp Boehm-Sturm[2,3], Peter Vajkoczy[1], Ran Xu[1]

[1]Department of Neurosurgery, Charité - Universitätsmedizin Berlin, corporate member of Freie Universität Berlin, and Humboldt-Universität zu Berlin, and Berlin Institute of Health, Berlin, Germany.

[2]Department of Experimental Neurology and Center for Stroke Research Berlin, Charité - Universitätsmedizin Berlin, corporate member of Freie Universität Berlin, Humboldt-Universität zu Berlin, and Berlin Institute of Health, Berlin, Germany.

[3]NeuroCure Cluster of Excellence and Charité Core Facility 7T Experimental MRIs, Charité – Universitätsmedizin Berlin, Berlin, Germany.

*Equal contribution

E-mail addresses of co-authors:

Shuheng Liu	(shuheng.liu@charite.de)
Katharina Tielking	(katharina.tielking@charite.de)
Dario von Wedel	(dario.von-wedel@charite.de)
Melina Nieminen-Kelhä	(melina.nieminen@charite.de)
Susanne Mueller	(susanne.mueller1@charite.de)
Philipp Boehm-Sturm	(philipp.boehm-sturm@charite.de)
Peter Vajkoczy	(peter.vajkoczy@charite.de)
Ran Xu	(ran.xu@charite.de)

Corresponding author:

Ran Xu	(ran.xu@charite.de)

SUMMARY:

Here we present a standardized SAH mouse model, induced by endovascular filament perforation, combined with magnetic resonance imaging (MRI) 24 h after operation to ensure the correct bleeding site and exclude other relevant intracranial pathologies.

ABSTRACT:

The endovascular filament perforation model to mimic subarachnoid hemorrhage (SAH) is a commonly used model – however, the technique can cause a high mortality rate as well as an uncontrollable volume of SAH and other intracranial complications such as stroke or intracranial hemorrhage. In this protocol, a standardized SAH mouse model is presented, induced by endovascular filament perforation, combined with magnetic resonance imaging (MRI) 24 h after operation to ensure the correct bleeding site and exclude other relevant intracranial pathologies.

Briefly, C57BL/6J mice are anesthetized with an intraperitoneal ketamine/xylazine (70 mg/16 mg/kg body weight) injection and placed in a supine position. After midline neck incision, the common carotid artery (CCA) and carotid bifurcation are exposed, and a 5-0 non-absorbable monofilament polypropylene suture is inserted in a retrograde fashion into the external carotid artery (ECA) and advanced into the common carotid artery. Then, the filament is invaginated into the internal carotid artery (ICA) and pushed forward to perforate the anterior cerebral artery (ACA). After recovery from surgery, mice undergo a 7.0 T MRI 24 h later. The volume of bleeding can be quantified and graded via postoperative MRI, enabling a robust experimental SAH group with the option to perform further subgroup analyses based on blood quantity.

INTRODUCTION:

Subarachnoid hemorrhage (SAH) is caused by the rupture of an intracranial aneurysm and poses a life-threatening emergency, associated with substantial morbidity and mortality, accounting for approx. 5% of strokes[1,2]. SAH patients present with severe headaches, neurological dysfunction, and progressive disturbance of consciousness[3]. Around 30% of SAH patients die within the first 30 days after the initial bleeding event[4]. Clinically, 50% of patients experience delayed brain injury (DBI) after early brain injury. DBI is characterized by delayed cerebral ischemia and delayed neurological deficits. Current studies have shown that the synergistic effects of several different factors lead to the loss of neurological function, including the destruction of the blood-brain barrier, the contraction of small arteries, microcirculatory dysfunction, and thrombosis[5,6].

One unique aspect of SAH is that the pathogenesis originates from an extraparenchymal location but then leads to detrimental cascades inside the parenchyma: the pathology begins with the accumulation of blood in the subarachnoid space, triggering a multitude of intraparenchymal effects, such as neuroinflammation, neuronal and endothelial cell apoptosis, cortical spreading depolarization, and brain edema formation[7,8].

Clinical research is limited by several factors, making the animal model a critical element in consistently and accurately mimicking the pathomechanistic changes of the disease. Different SAH model protocols have been proposed, e.g., autologous blood injection into the cisterna magna (ACM). Also, a modified method with a double injection of autologous blood into the cisterna magna and optic chiasm cistern (APC) respectively[9,10]. While autologous blood injection is a simple way to simulate the pathological process of vasospasm and inflammatory reactions after subarachnoid hemorrhage, the following rise of intracranial pressure (ICP) is relatively slow, and no noteworthy changes in the permeability of the blood-brain barrier are induced[11,12]. Another method, the periarterial blood placement, usually used in large SAH models (e.g., monkeys and dogs), involves placing anticoagulated autologous blood or comparable blood products around the vessel. The diameter changes of the artery can be observed with a microscope, serving as an indicator for cerebral vasospasm after SAH[13].

Barry et al. first described an endovascular perforation model in 1979 in which the basilar artery is exposed after removing the skull; the artery is then punctured with tungsten microelectrodes, using a microscopic stereotactic technique[14]. In 1995, Bederson and Veelken modified the Zea-Longa model of cerebral ischemia and established the endovascular perforation, which has

been continuously improved ever since[15,16]. This method is based on the fact that mice and humans share a similar intracranial vascular network, known as the circle of Willis.

For postoperative evaluation and grading of SAH in the mouse model, different approaches have been proposed. Sugawara et al. developed a grading scale that has been widely used since 2008[17]. This method assesses the severity of SAH based on morphological changes. However, for this method, the mouse's brain tissue morphology must be examined under direct vision, and therefore, the mouse must be sacrificed for assessment. Furthermore, several methods for determining SAH severity *in vivo* have been established. Approaches range from simple neurological scoring to monitoring of intracranial pressure (ICP) to various radiological imaging techniques. Furthermore, MRI grading has been shown as a new, non-invasive tool to grade SAH severity, correlating to neurological score[18,19].

Here, a protocol for an SAH model caused by endovascular perforation is presented, combined with postoperative MRI. In an attempt to establish a system to objectify the amount of bleeding in an *in vivo* setting, we also developed a system for SAH grading and quantification of total blood volume based on 7.0 T high-resolution T2-weighted MRI. This approach ensures the correct induction of SAH and exclusion of other pathologies such as stroke, hydrocephalus, or intracerebral hemorrhage (ICH) and complications.

PROTOCOL:

The experiments were performed in accordance with the guidelines and regulations set forth by Landesamt fuer Gesundheit und Soziales (LaGeSo), Berlin, Germany (G0063/18). In this study, C57Bl/6J male (8–12 weeks old) mice with a weight of 25 ± 0.286 g (average ± s.e.m.) were used.

1. Animal preparation

1.1. Induce anesthesia by injecting ketamine (70 mg/kg) and xylazine (16 mg/kg) intraperitoneally. Maintain normal body temperature, contributing to quick induction of deep anesthesia. Test for adequate sedation with a pain stimulus, such as a toe pinch, and verify the absence of a reaction.

1.2. Carefully shave the neck hair of the mouse with a razor, clean it with 70% ethanol, and apply 1% lidocaine on the skin surface.

1.3. Place the mouse in a supine position. Use tape to fix the limbs and tail, gently stretching the skin of the neck to the opposite side of the surgery. Simultaneously, elevate the neck slightly.

1.4. Use ophthalmic ointment (e.g., 5% dexpanthenol) to prevent dehydration of the eyes during the operation.

2. SAH induction

[Place **Figure 1** here]

2.1. Open the neck skin with a sterile scalpel, from the chin to the upper edge of the breastbone (1.5 cm), and bluntly separate salivary glands from their surrounding connective tissue.

2.2. Separate the muscle group along one side [in this case, the right side] of the trachea, exposing the common carotid artery (CCA) sheath covered with nourishing blood vessels and venules. The CCA and the vagal nerve are located in close proximity to each other.

2.3. Dissociate the CCA and leave a free 5-0 silk suture around the CCA without ligating it in advance. Pay attention to the protection of the vagal nerve, as it is easily damaged (**Figure 1A**).

2.4. A triple bifurcation of the CCA, the ICA, and the ECA is visible along the lower posterior third of the diastasis. Dissect the distal end of the ECA and ligate the vessel twice as far proximally as possible. Prearrange one ligation for the filament around the ECA stump, do not close it until successful filament insertion.

2.5. Disconnect the ECA at the midpoint of the twice ligated segment, creating a vessel stump.

2.6. Use a suture or micro clip to occlude the ICA and CCA temporarily (**Figure 1B**).

2.7. Make a small incision (approximately half of the ECA diameter) in the ECA using microvascular scissors. Insert a 5-0 prolene filament into the ECA and advance it into the CCA.

2.8. Close the ligature on the ECA slightly while loosening the micro clip on the ICA and CCA (**Figure 1C**).

2.9. Gently pull back on the filament and adjust the ECA stump in the cranial direction, invaginating the filament through the bifurcation into the ICA (**Figure 1D**).

2.10. Point the filament tip medially at an angle of ~30° to the tracheal midline and ~30° to the horizontal plane. Push the filament forward inside the ICA. After reaching the ACA-MCA bifurcation, resistance is encountered (~9 mm).

2.11. Advance the filament 3 mm further, perforating the right ACA. Promptly withdraw the filament to the ECA stump, allowing blood flow into the subarachnoid space.

2.12. Keep the filament in this position for about 10 s (**Figure 1E**). The presence of muscle tremors, ipsilateral miosis, tidal breathing, altered heart rhythm, and urinary incontinence can be supporting evidence of successful surgery.

2.13. Pull out the filament instantly and ligate the ECA with the prearranged suture. Reopen the CCA and allow reperfusion and further effusion of blood into the subarachnoid space (**Figure 1F**).

2.14. After checking for bleeding leakage, disinfect the skin again and suture the wound.

2.15. Place the mouse in a thermal box until consciousness is regained. Wait until the animal is fully awake and ensure it has regained sufficient consciousness to maintain sternal recumbency. Do not return animals to the company of other mice until fully recovered.

2.16. Administer 1.2 mg/mL paracetamol to the drinking water for pain relief.

2.17. Check on the mice daily after surgery.

3. MRI measurement

3.1. 24 h after surgery, perform MRI using a rodent scanner (**Table of Materials**) and a dedicated mouse head resonator – here, a 20 mm transmit/receive quadrature volume resonator was used.

3.2. Place the mouse on a heated circulating water blanket to ensure a constant body temperature of ~37 °C. Induce anesthesia with 2.5 % isoflurane in an O2/N2O mixture (30%/70%) and maintain with 1.5–2 % isoflurane via facemask under continuous ventilation monitoring.

3.3. First perform a fast reference scan acquiring 3 orthogonal slice packages (Tri-Pilot-Multi, FLASH with repetition time TR/echo time TE = 200 ms/3 ms, 1 average, flip angle FA = 30°, field of view FOV = 28 mm x 28 mm, matrix MTX = 256 x 256, slice thickness 1 mm, total acquisition time TA =30 s).

3.4. Then use a high resolution T2-weighted 2D turbo spin-echo sequence for imaging (imaging parameters TR/TE = 5505 ms/36 ms, RARE factor 8, 6 averages, 46 contiguous axial slices with a slice thickness of 0.35 mm to cover the whole brain, FOV = 25.6 mm x 25.6 mm, MTX = 256 x 256, TA = 13 min).

3.5. If the result is unclear, use an additional respiration triggered T2*weighted gradient echo sequence with the same isodistance as the T2w scan (2D FLASH, TR/TE = 600 ms/6.3 ms, FA = 30°, 1 average, 20 axial slices with 0.35 mm thickness, FOV and MTX identical to T2w, TA = 5–10 min depending on the respiration rate).

3.6. Transfer the data into the DICOM image format and use ImageJ software for SAH grading and volumetry of blood clots. Details on the quantification are listed as a step-by-step guide in the supplementary material (**Supplementary Figure 1**).

REPRESENTATIVE RESULTS:

Mortality

For this study, a total of 92 male C57Bl/6J mice aged between 8–12 weeks were subjected to SAH operation; in these, we observed an overall mortality rate of 11.9% (n = 12). Mortality occurred exclusively within the first 6–24 h after surgery, suggesting perioperative mortality as well as SAH bleeding itself as the most likely contributing factors.

SAH bleeding grade

A total of 50 mice received MRI 24 h postoperatively to confirm SAH and ensure the detection of other co-occurring pathologies, including subacute ischemic stroke and hydrocephalus. The remaining animals were used for earlier scans to select the adequate time for postoperative MRI. Among the 50 examined mice at 24 h time point, n = 7 animals that did not present SAH (bleeding grade 0) and n = 5 mice in which additional stroke and/or ICH (bleeding grade IV) was detected. The SAH bleeding grade was quantified based on T2 weighted MRI scans as follows (**Figure 2A**,**B**):

grade 0: no SAH or hemorrhage identified (14%)
grade I: SAH thickness ≤0.80 mm (24%)
grade II: SAH thickness >0.8 and <1.6 mm (28%)
grade III: SAH thickness ≥1.6 mm (24%)
grade IV: SAH with either ICH and/or stroke (10%).

[Place **Figure 2** here]

Bleeding volume

For grade I-III, bleeding volume was quantified by two different methods:

Method A: The total volume of bleeding was calculated based on the abc/2 volume estimation by Kathari et al., a modification of the equation for ellipsoid volume which has been utilized widely in the clinical setting to estimate ICH volume (**Figure 2D**)[20].

Method B: The calculated SAH bleeding volume was estimated based on the formula $V = (A_1 + A_2 + \cdots + A_x) \cdot d$, by which the bleeding area was determined via ImageJ on each slide section and the sum of all bleeding areas were multiplied with the corresponding MRI slide thickness ('A_i' corresponds to the bleeding area on slice 'i', 'x' is the total number of slices, 'd' corresponds to the slice thickness). This method took the irregularity of the shape into account (**Figure 2C**,**E**). Expectedly, Method B showed a bigger range of values in each subgroup. However, both methods showed a significant difference in the corresponding bleeding grades that were based on the axial SAH thickness and are described in the following paragraph. **Supplementary Figure 2** shows the SAH volume of all subgroups; expectedly, grade IV was of heterogeneous nature since it contained co-occurring ICH as well.

Statistical analysis and figures

Data were analyzed using GraphPad Prism for statistical analyses. One-way ANOVA analyses were used to compare multiple groups. The values are displayed as means ± standard errors and p-values of $p < 0.05$ were considered statistically significant. Elements of **Figure 1** and **Figure 2** were composed using BioRender.com.

FIGURE AND TABLE LEGENDS:

Figure 1: Step-by-step images of surgical technique. (**A**) Depiction of the exposed right carotid artery anatomy: the CCA and its bifurcation into ICA and ECA are identified, as well as the small branches of the ECA (OA and STA). (**B**) The ECA is mobilized from the surrounding tissue and ligated with two sutures before cutting it. A third ligation needs to be placed loosely near the bifurcation without occluding it. (**C**) The ICA and CCA are occluded temporarily (with either ligation or clips) to prevent excessive bleeding when the ECA is carefully incised. (**D**) The filament is inserted into the ECA and advanced into the CCA. The prearranged ligation must be tightened carefully so that no blood effusion occurs but advancing the filament remains possible. (**E**) The ICA and CCA are reopened, and the ECA stump needs to be adjusted to a cranial direction. By pushing the filament ~9 mm forward into the ICA, the ACA-MCA bifurcation will be reached, and the vessel is then perforated by pushing the filament ~3mm further. (**F**) The filament is withdrawn after ensuring a temporal re-ligation of the CCA. The prearranged ligation of the ECA is quickly occluded, and the CCA is reopened to allow reperfusion. Abbreviations: ACA = anterior cerebral artery, CCA = common carotid artery, ECA = external carotid artery, MCA = middle cerebral artery, ICA = internal carotid artery, OA = occipital artery, PPA = pterygopalatine artery, STA = superior thyroid artery. Scale bar = 2 mm.

Figure 2: SAH grading system with corresponding blood volume and MRI images. (**A**) Total bleeding volume of each SAH grade based on the Kothari abc/2 volume estimation. (**B**,**C**) Calculated SAH bleeding volume based on the formula $V = (A_1 + A_2 + \cdots + A_x) \cdot d$, by which the bleeding area is determined via ImageJ on each slide section, and the sum of all bleeding areas is multiplied with the corresponding MRI slide thickness. Values are expressed as mean ± SEM. (**D**) Pie chart showing the distribution of SAH grade in the experimental mice. (**E**) T2-weighted MRI axial sections depicting representative images categorizing SAH grade. Grade 0: no SAH or hemorrhage identified (14%); grade I: SAH thickness ≤0.80 mm; grade II: SAH thickness >0.8 and <1.6 mm; grade III: SAH thickness ≥1.6 mm; grade IV: SAH with either ICH and/or stroke. Abbreviations: ICH = intracerebral hemorrhage, MRI = magnetic resonance imaging. Scale bar = 5 mm.

Figure 3: Mouse brain anatomy and macroscopic images of SAH. (A) Schematic mouse vascular anatomy showing site of filament perforation. (**B**) Classical macroscopic image of successful induction of SAH. Before removing the brain, a perfusion of 1x PBS was performed. (**C**) Macroscopic view of the mouse in which the filament was pushed too deep, causing ICH. Abbreviations: ACA = anterior cerebral artery, ECA = external carotid artery, CCA = common carotid artery, ICA = internal carotid artery, ICH = intracerebral hemorrhage, L = left, MCA = middle cerebral artery, PPA = pterygopalatine artery, R = right. Scale bar = 3 mm.

Supplemental Figure 1: A step-by-step guide for quantifying bleeding volume with ImageJ. Import the images with ImageJ, and enter “Strg+I” to show the dimensional data. Then set the scale for the image. Identify all the images in which SAH can be seen. For method A, identify the slice with the biggest bleeding area and measure the craniocaudal length *(=a)* as well as the mediolateral length *(=b)* of the two orthogonal axes that span the ellipsoid SAH volume. The

ventrodorsal dimension *(=c)* of the ellipsoid shape can be estimated based on the slice thickness and the number of slices on which SAH is seen [c = slice thickness x number of slices]. Calculate the volume based on the formula: *V= abc/2.* For method B, measure the bleeding areas on each slice separately and then calculate the volume based on the formula: $V = (A_1 + A_2 + \cdots + A_x) \cdot d$, by which *d= slice thickness*.

Supplemental Figure 2: Bleeding volumes of all subgroups. (**A**) Bleeding volume (mm^3) in each subgroup based on method A using the formula *V= abc/2*. (**B**) Bleeding volumes (mm^3) of the corresponding subgroups using method B (formula $V = (A_1 + A_2 + \cdots + A_x) \cdot d$; *d= slice thickness*).

DISCUSSION:

In summary, a standardized SAH mouse model induced by endovascular filament perforation operation is presented with minor invasion, short operative time, and acceptable mortality rates. MRI is conducted 24 h postoperatively to ensure the correct bleeding site and the exclusion of other relevant intracranial pathologies. Furthermore, we classified different SAH bleeding grades and measured bleeding volumes, allowing further subgroup analyses based on bleeding grade.

Adequate positioning of the mouse affects the success of the correct perforation. The mouse's neck should be stretched slightly to the opposite side of the operation, with the head being slightly elevated. This exposes the trifurcation and makes the puncture path easier accessible. If advancing of the filament fails, it can be helpful to withdraw the filament slightly to the trifurcation and adjust the head's position until advancing is possible without any resistance.

Intraoperative nerve protection is critical. Disturbances of the vagal nerve and cervical plexus can cause changes in respiratory and cardiac rhythms, and some mice may even die because of malignant arrhythmias. If these symptoms occur, it is essential to pause the procedure for a few minutes until the breathing and heart rate stabilize.

Reducing intraoperative blood loss is vital for improving the survival of mice. Based on our experience, double suture ligation is best applied close to the ECA. We disconnect the ECA in the middle of the two ligations to prevent blood backflow from the distal ECA stump. When the filament is inserted into the ECA, the prearranged suture should be ligated to prevent blood effusion from the incision. It is critical not to ligate the vessel too tightly as this hinders proper filament advancement.

Appropriate depth of filament insertion is essential for successful SAH induction. Due to the age of the mice used (8–12 weeks), we insert the filament ~9 mm inside the ICA and stop when resistance was encountered, then advanced ~3 mm further for perforation. Inserting the filament not deep enough could result in insufficient perforation, causing no SAH, whereas excessive insertion might lead to stroke and/or ICH (**Figure 3**). At the same time, the mice's original anatomy and vascular structures need to be preserved as well as possible during the operation. For example, the occipital artery (OA) or superior thyroid artery (STA), and nourishing blood vessels on the sheath, should be retained as much as possible.

[Place **Figure 3** here]

The endovascular perforation model is a commonly used animal model to study SAH but the means to ensure bleeding grade and exclude other pathologies such as stroke or intracerebral hemorrhage are not sufficiently standardized in the literature[21]. Just like any operative animal model, the success rate and robustness of SAH induction depend on the experience of the surgeon.

Currently, the endovascular perforation model is one of the most popular methods of experimental SAH induction in mice. This approach does not require craniotomy and accurately resembles the processes taking place in humans suffering from aneurysmal SAH[22]. Advantages include close imitation of the pathophysiology following aneurysmal SAH, regarding acute and delayed reactions[23]. Additionally, mortality rates in this model have been shown to be similar to those of clinical studies in patients suffering from aneurysmal SAH[23]. In comparison to blood injection models, changes in blood-brain barrier permeability are more closely mimicked, and higher rates of vasospasm are achieved in filament perforation[11,24]. Blood injection models are more invasive and therefore pose a greater risk for tissue damage when compared to the less invasive endovascular perforation model. Nonetheless, it should be noted that a major advantage of blood injection methods is the easily controlled blood volume[23]. The standardization of injection speed is important to consider since alterations of ICP are heavily dependent on the speed of injection[23]. Apart from these classical models, the combination of elastase injection to induce aneurysm formation and hypertension by unilateral nephrectomy, ultimately leading to aneurysm rupture, poses an interesting model to study subarachnoid hemorrhage in a more pathophysiologically realistic setting[25]. Integrating such techniques with genetically modified mice will be of interest for future studies.

Previous SAH grading systems for the filament perforation model are based on the amount of visible subarachnoid blood in different brain segments after the mouse has been sacrificed[17]. Consequently, these grading systems do not allow long-term studies when the blood has been already resorbed at the time of sacrification. In the clinical setting, SAH is graded based on clinical presentation as well SAH thickness on imaging, corresponding to clinical outcome[1,26–28]. Hence, in an attempt to classify the bleeding severity noninvasively, we added a standardized MRI follow-up examination to grade SAH radiographically, by which the grading was based on pre-existing human grading scales, adapting the grading system of a previously published MRI grading system in SAH mice by Egashira et al.[18]. This approach also ensures quantification of total blood volume and exclusion of animals with other co-occurring intracranial pathologies (e.g., stroke, ICH, hydrocephalus). Some studies proposed intracranial pressure (ICP), cerebral perfusion, and blood pressure monitoring as evidence of successful SAH induction, which might be additional helpful tools[29]. Indirect ways to grade the severity of SAH and potential intraparenchymal damage include combining clinical findings with histological staining for cell death markers such as p53, TUNEL or caspase-3. However, these indirect tools such as ICP monitoring as well as neurological may not distinguish neatly other pathologies such as stroke, intracranial hemorrhage, or hydrocephalus. Despite the advantages of MRI grading, there is one major

drawback of this approach regarding its feasibility: MRI is not as widely available to laboratories as other methods. This limits the broad introduction of MRI grading systems in experimental SAH. When available, however, the presented MRI grading system adds a tool to standardize experimental SAH models, therefore facilitating reproducibility and comparability of the experiments[23]. In this study, despite observed clinical changes during the operation, there was still a 14% rate of mice without evidence of SAH on postoperative MRI. Possibly, mice in this subgroup suffered from microhemorrhages, not detectable on MRI (similar to SAH patients with negative CT but the presence of xanthochromia in lumbar puncture). These mice were excluded in this experimental setup for further analyses. The technical reason for these "no-bleeds" on MRI could be insufficient filament insertion, resulting in no perforation (e.g., by incorrect placement into OA or pterygopalatine artery (PPA)). Additionally, the successfully perforated vessel might close again after withdrawal of the filament, preventing SAH.

In summary, a standardized model for experimental aneurysmal SAH by endovascular perforation is presented, combined with MR imaging 24 h after surgery to confirm and grade the bleeding and to exclude other relevant intracranial pathologies.

ACKNOWLEDGMENTS:

SL was supported by the Chinese Scholarship Council. KT was supported by the BIH-MD scholarship of the Berlin Institute of Health and the Sonnenfeld-Stiftung. RX is supported by the BIH-Charité Clinician Scientist Program, funded by the Charité –Universitätsmedizin Berlin and the Berlin Institute of Health. We acknowledge support from the German Research Foundation (DFG) and the Open Access Publication Fund of Charité – Universitätsmedizin Berlin.

DISCLOSURES:

No conflicts of interest

REFERENCES:

1. Macdonald, R. L., Schweizer, T. A. Spontaneous subarachnoid haemorrhage. *The Lancet*. **389** (10069), 655–666 (2017).
2. van Gijn, J., Kerr, R. S., Rinkel, G. J. Subarachnoid haemorrhage. *The Lancet*. **369** (9558), 306–318 (2007).
3. Abraham, M. K., Chang, W. -T. W. Subarachnoid hemorrhage. *Emergency Medicine Clinics of North America*. **34** (4), 901–916 (2016).
4. Schertz, M., Mehdaoui, H., Hamlat, A., Piotin, M., Banydeen, R., Mejdoubi, M. Incidence and mortality of spontaneous subarachnoid hemorrhage in martinique. *PLOS ONE*. **11** (5), e0155945 (2016).
5. Okazaki, T., Kuroda, Y. Aneurysmal subarachnoid hemorrhage: intensive care for improving neurological outcome. *Journal of Intensive Care*. **6** (1), 28 (2018).
6. Kilbourn, K. J., Levy, S., Staff, I., Kureshi, I., McCullough, L. Clinical characteristics and outcomes of neurogenic stress cadiomyopathy in aneurysmal subarachnoid hemorrhage. *Clinical Neurology and Neurosurgery*. **115** (7), 909–914 (2013).
7. de Oliveira Manoel, A. L. et al. The critical care management of spontaneous intracranial hemorrhage: a contemporary review. *Critical Care*. **20** (1), 272 (2016).

8. Schneider, U. C. et al. Microglia inflict delayed brain injury after subarachnoid hemorrhage. *Acta Neuropathologica*. **130** (2), 215–231 (2015).
9. Delgado, T. J., Brismar, J., Svendgaard, N. A. Subarachnoid haemorrhage in the rat: angiography and fluorescence microscopy of the major cerebral arteries. *Stroke*. **16** (4), 595–602 (1985).
10. Piepgras, A., Thomé, C., Schmiedek, P. Characterization of an anterior circulation rat subarachnoid hemorrhage model. *Stroke*. **26** (12), 2347–2352 (1995).
11. Suzuki, H. et al. Heme oxygenase-1 gene induction as an intrinsic regulation against delayed cerebral vasospasm in rats. *Journal of Clinical Investigation*. **104** (1), 59–66 (1999).
12. Dudhani, R. V., Kyle, M., Dedeo, C., Riordan, M., Deshaies, E. M. A Low mortality rat model to assess delayed cerebral vasospasm after experimental subarachnoid hemorrhage. *Journal of Visualized Experiments: JoVE*. **71**, 4157 (2013).
13. Iuliano, B. A., Pluta, R. M., Jung, C., Oldfield, E. H. Endothelial dysfunction in a primate model of cerebral vasospasm. *Journal of Neurosurgery*. **100** (2), 287–294 (2004).
14. Barry, K. J., Gogjian, M. A., Stein, B. M. Small animal model for investigation of subarachnoid hemorrhage and cerebral vasospasm. *Stroke*. **10** (5), 538–541 (1979).
15. Bederson, J. B., Germano, I. M., Guarino, L. Cortical blood flow and cerebral perfusion pressure in a new noncraniotomy model of subarachnoid hemorrhage in the rat. *Stroke*. **26** (6), 1086–1092 (1995).
16. Veelken, J. A., Laing, R. J. C., Jakubowski, J. The Sheffield model of subarachnoid hemorrhage in rats. *Stroke*. **26** (7), 1279–1284 (1995).
17. Sugawara, T., Ayer, R., Jadhav, V., Zhang, J. H. A new grading system evaluating bleeding scale in filament perforation subarachnoid hemorrhage rat model. *Journal of Neuroscience Methods*. **167** (2), 327–334 (2008).
18. Egashira, Y., Shishido, H., Hua, Y., Keep, R. F., Xi, G. New grading system based on magnetic resonance imaging in a mouse model of subarachnoid hemorrhage. *Stroke*. **46** (2), 582–584 (2015).
19. Mutoh, T., Mutoh, T., Sasaki, K., Nakamura, K., Taki, Y., Ishikawa, T. Value of three-dimensional maximum intensity projection display to assist in magnetic resonance imaging (MRI)-based grading in a mouse model of subarachnoid hemorrhage. *Medical Science Monitor*. **22**, 2050–2055 (2016).
20. Kothari, R. U. et al. The ABCs of measuring intracerebral hemorrhage volumes. *Stroke*. **27** (8), 1304–1305 (1996).
21. Leclerc, J. L. et al. A comparison of pathophysiology in humans and rodent models of subarachnoid hemorrhage. *Frontiers in Molecular Neuroscience*. **11**, 71 (2018).
22. Titova, E., Ostrowski, R. P., Zhang, J. H., Tang, J. Experimental models of subarachnoid hemorrhage for studies of cerebral vasospasm. *Neurological Research*. **31** (6), 568–581 (2009).
23. Marbacher, S. et al. Systematic review of in vivo animal models of subarachnoid hemorrhage: Species, standard parameters, and outcomes. *Translational Stroke Research*. **10** (3), 250–258 (2019).
24. Marbacher, S., Fandino, J., Kitchen, N. D. Standard intracranial in vivo animal models of delayed cerebral vasospasm. *British Journal of Neurosurgery*. **24** (4), 415–434 (2010).
25. Thompson, J. W. et al. In vivo cerebral aneurysm models. *Neurosurgical Focus*. **47** (1), 1–8 (2019).

26. Frontera, J. A. et al. Prediction of symptomatic vasospasm after subarachnoid hemorrhage: The modified fisher scale. *Neurosurgery*. **59** (1), 21–26 (2006).
27. Fisher, C. M., Kistler, J. P., Davis, J. M. Relation of cerebral vasospasm to subarachnoid hemorrhage visualized by computerized tomographic scanning. *Neurosurgery*. **6** (1), 1–9 (1980).
28. Wilson, D. A. et al. A simple and quantitative method to predict symptomatic vasospasm after subarachnoid hemorrhage based on computed tomography: Beyond the fisher scale. *Neurosurgery*. **71** (4), 869–875 (2012).
29. Schüller, K., Bühler, D., Plesnila, N. A murine model of subarachnoid hemorrhage. *Journal of Visualized Experiments: JoVE*. **81**, 50845 (2013).

Figure 1

Click here to access/download;Figure;Figures RX-1.pdf

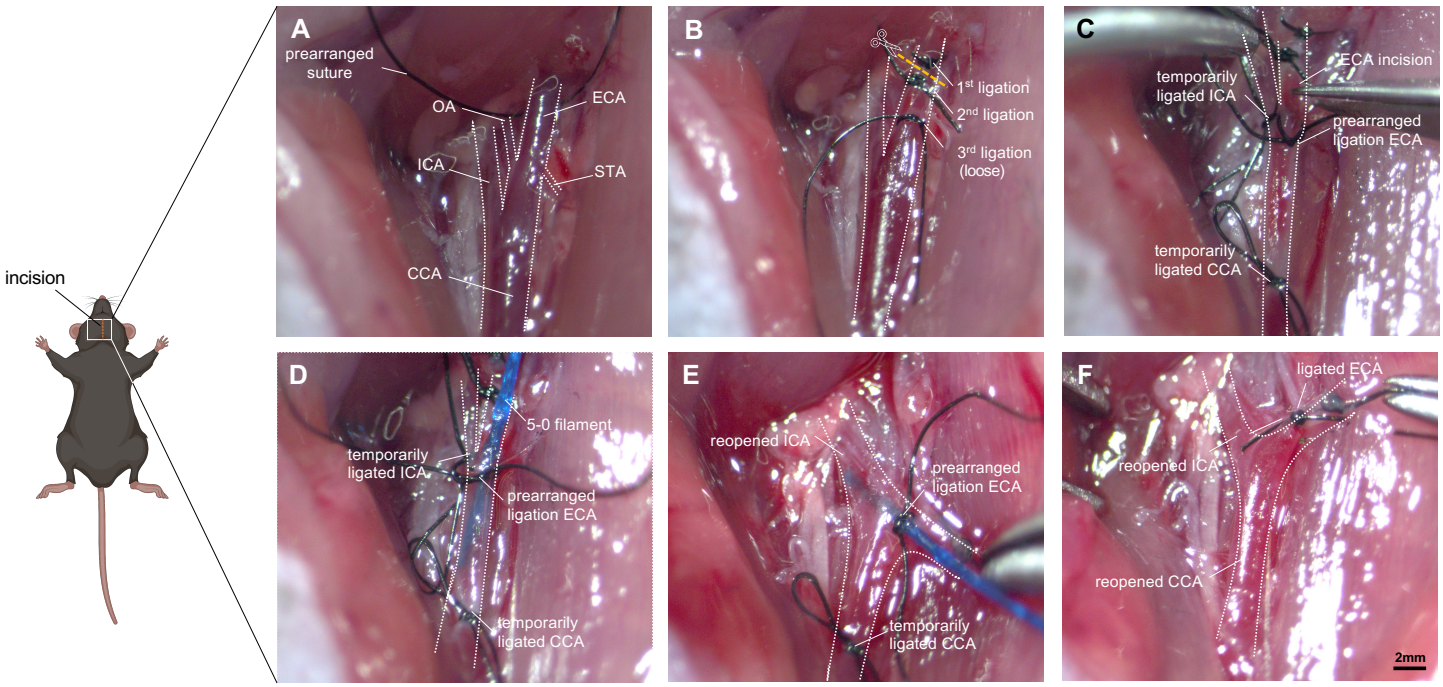

Figure 2

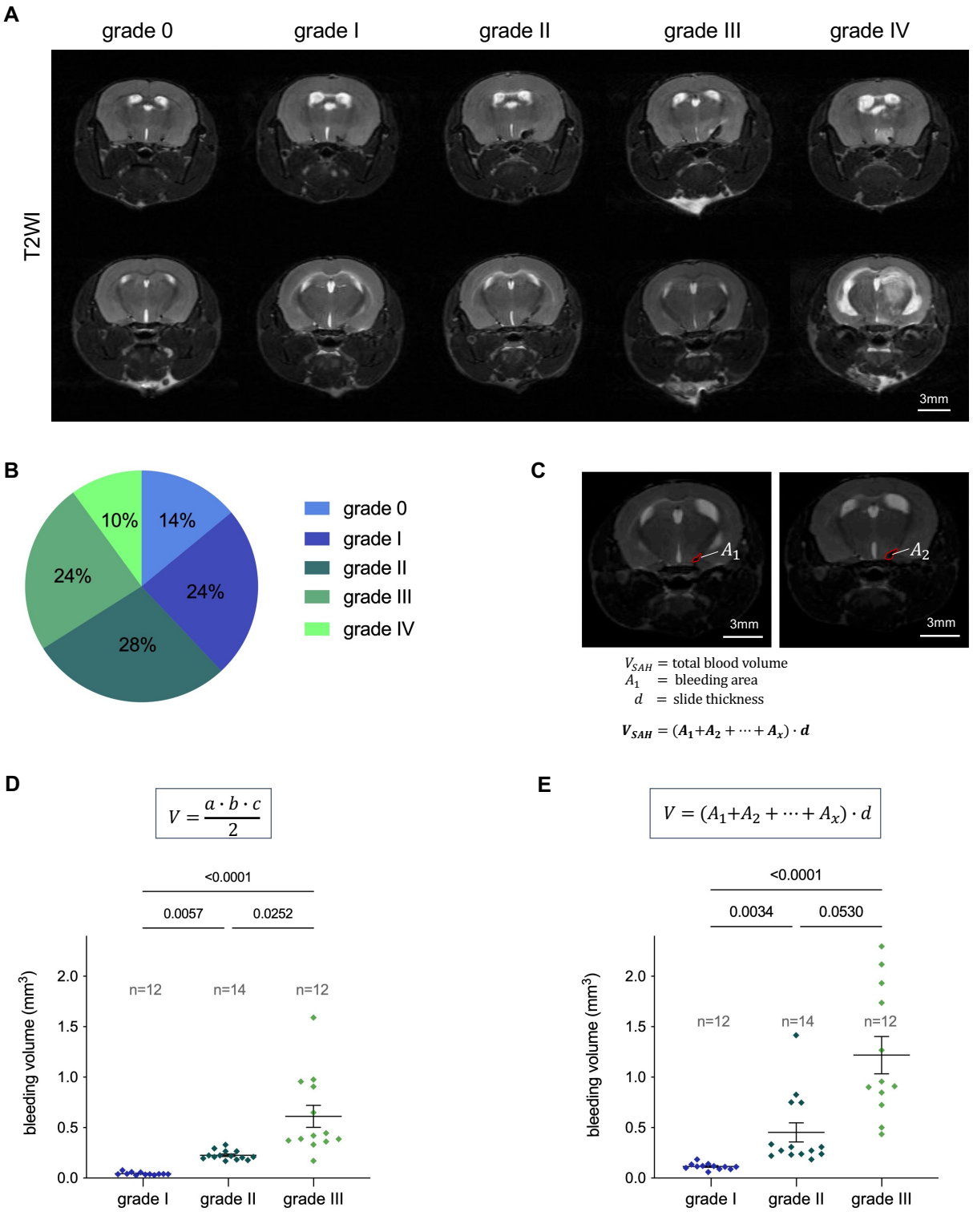

Figure 3

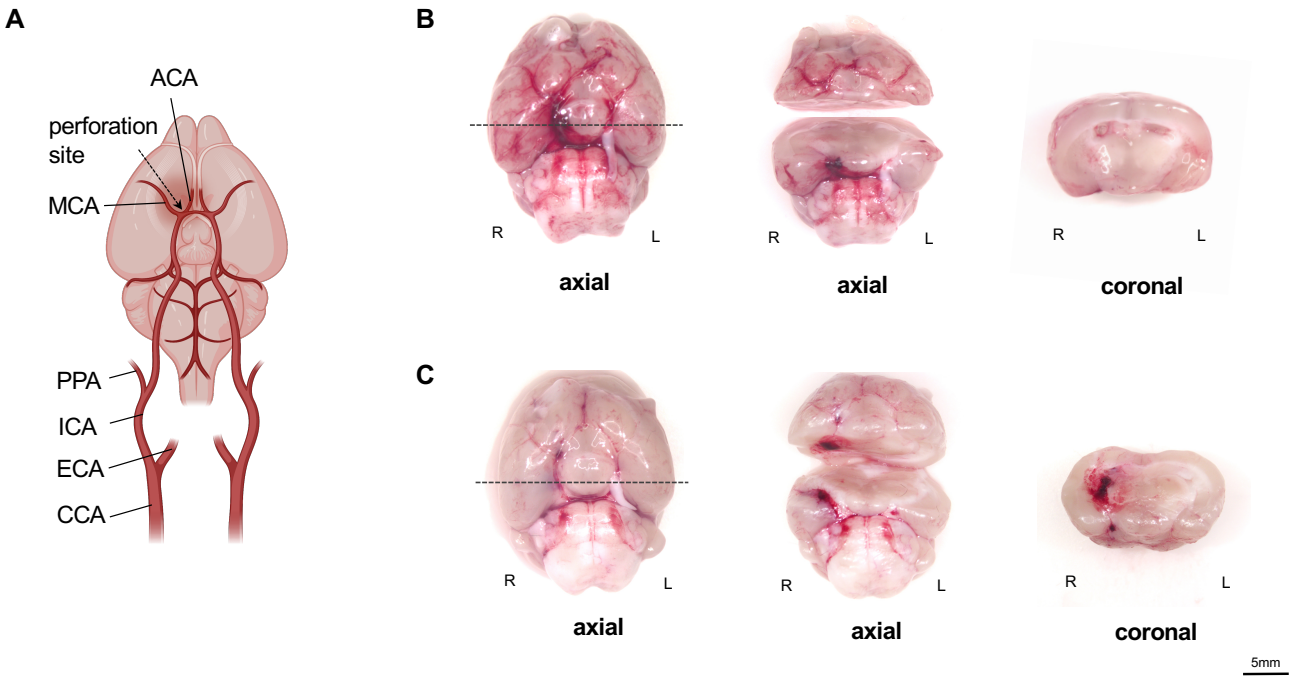

Response to Reviewers' Comments

Title: Endovascular perforation model for subarachnoid hemorrhage combined with Magnetic Resonance Imaging (MRI)

Journal of Visualized Experiments
Research Topic: Current methods in preclinical aneurysm models

Dear Editor,

Thank you for providing us with the opportunity to submit a revised version of our research article entitled "Endovascular perforation model for subarachnoid hemorrhage combined with Magnetic Resonance Imaging (MRI)". We have addressed the reviewers' concerns in an itemized, point-by-point response.

We are looking forward to hearing from you soon and appreciate your attention. Please contact us at any time should you require additional information.

Sincerely,

Dr. Ran Xu
Department of Neurosurgery
Charité University Hospital
Charitéplatz 1
10117 Berlin
Germany

Author's Revision Letter

Title: Endovascular perforation model for subarachnoid hemorrhage combined with Magnetic Resonance Imaging (MRI)

We would like to thank the Editor and reviewers for their thoughtful and constructive suggestions that helped elevate the quality and clarity of the manuscript. Please find in the following itemized point-by-point answers to the reviewers' concerns. All changes within the revised manuscript are highlighted in red for easier reviewing.

Editorial comments

1. Please take this opportunity to thoroughly proofread the manuscript to ensure that there are no spelling or grammar issues.

We proofread the manuscript and double-checked for spelling and grammar issues.

2. Please revise the following lines to avoid previously published work: 46-49, 93-97.

The aforementioned lines were revised accordingly.

3. Please use SI units as much as possible and abbreviate all units: L, mL, µL, cm, kg, etc. Use h, min, s, for hour, minute, second. Include a space between all numbers and the corresponding unit: 50 mg, 100 mL, 37 °C, etc.

The SI units were changed as requested and marked in red.

4. JoVE cannot publish manuscripts containing commercial language. This includes trademark symbols (™), registered symbols (®), and company names before an instrument or reagent. Please remove all commercial language from your manuscript and use generic terms instead. All commercial products should be sufficiently referenced in the Table of Materials.

All commercial language content was removed in the manuscript.

5. For example, 5% dexpanthenol, Bayer, Germany, Pharmascan 70/16, Bruker, Ettlingen, Germany, Bruker Paravision 5.1 software, Graphpad Software, Version 9.0, etc.

As mentioned before, all content involving commercial language was revised in the manuscript.

6. Please revise the text to avoid the use of any personal pronouns (e.g., "we", "you", "our" etc.).

Personal pronouns were modified and replaced in the paper.

7. Please include an ethics statement before your numbered protocol steps, indicating that the protocol follows the animal care guidelines of your institution.

Ethics statement about the mouse care and institution was added in the protocol part: "*The experiments were performed in accordance with the guidelines and regulations set forth by Landesamt fuer Gesundheit und Soziales (LaGeSo), Berlin, Germany (G0063/18).*"

8. Please adjust the numbering of the Protocol to follow the JoVE Instructions for Authors. For example, 1 should be followed by 1.1 and then 1.1.1 and 1.1.2 if necessary.

The numbering of the protocol was corrected according to the above-suggested style.

9. The Protocol should be made up almost entirely of discrete steps without large paragraphs of text between sections. Please simplify the Protocol so that individual steps contain only 2-3 actions per step and a maximum of 4 sentences per step.

The sentences used to describe the protocol were revised accordingly. We also simplified the protocol with each step now containing not more than 2-3 actions.

10. Please add more details to your protocol steps. Please ensure you answer the “how” question, i.e., how is the step performed?

Line 116: Please mention how proper anesthetization is confirmed.

We added this sentence to the protocol step: *“Test for adequate sedation with a pain stimulus, such as a toe pinch, and verify the absence of a reaction.”*

Line 136: What is the suture size?

Suture size was added to the manuscript (5-0 prolene).

Line 145: Please specify the incision size.

Incision size (half of the diameter of the ECA) was defined in the manuscript.

Line 163: For survival strategies, discuss post-surgical treatment of animals, including recovery conditions. Discuss maintenance of sterile conditions during survival surgery. Please specify that the animal is not left unattended until it has regained sufficient consciousness to maintain sternal recumbency. Please specify that the animal that has undergone surgery is not returned to the company of other animals until fully recovered.

Thank you for the important point made here. Survival strategies were added to the manuscript. Also, the protocol was adjusted in order to clarify that the operative technique is performed under sterile conditions. Mouse recovery conditions and postoperative care were specified in the manuscript: *“Place the mouse in a thermal box until consciousness is regained. Wait until the animals are fully awake and make sure they have regained sufficient consciousness to maintain sternal recumbency. Do not return animals to the company of other mice until fully recovered. Administer 1.2 mg/ml paracetamol to the drinking water for pain relief. Check mice daily after surgery.“*

11. Line 175, 179: Please elaborate on the steps for performing MRI. How were the images analyzed? Please include all analysis steps, how the data was retrieved, how was grading and volumetry analysis done, what parameters were used, etc. Please make sure to provide all the details such as “click this”, “select that”, “observe this”, etc. Please mention all the steps that are necessary to execute the action item. Please provide details so a reader may replicate your analysis including instrument settings, inputs, screenshots, etc. Readers of all levels of experience and expertise should be able to follow your protocol.

We added a supplementary figure with a step-by-step guide on the quantification method so the analysis can be easily replicated using freeware (ImageJ). Details are listed in the supplementary figure. If this should be also included as part of the video, we can provide the images as screenshots (they are now embedded in the figures) separately as well.

12. Line 199: Is A1, A2, etc. the bleeding area? Is d the sum of all bleeding areas? If yes, please specify this for clarity.

A1, A2, etc. corresponds to the the sum of all bleeding areas, d corresponds to the slide thickness – the manuscript was revised accordingly to specify this aspect.

13. Please include a single line space between all the steps, sub-steps, and notes. Please highlight up to 3 pages of the Protocol (including headings and spacing) that identifies the essential steps of the protocol for the video, i.e., the steps that should be visualized to tell the

most cohesive story of the Protocol. Remember that non-highlighted Protocol steps will remain in the manuscript, and therefore will still be available to the reader.

We have highlighted the protocol (in yellow) throughout the manuscript identifying the essential steps for the video.

14. Please do not number the representative results.

The numbering has been removed from the representative results section.

15. In the Representative Results please explain results obtained in the context of the technique you have described, e.g., how do these results show the technique, suggestions about how to analyze the outcome, etc. Please discuss all figures in the results section.

The representative results section was revised accordingly, and all the figures with representative results are discussed in the results section.

16. As we are a methods journal, please revise the Discussion to explicitly cover the following in detail in 3-6 paragraphs with citations:
(a) Any modifications and troubleshooting of the technique
(b) Any limitations of the technique
(c) The significance with respect to existing methods
(d) Any future applications of the technique

Limitation and weaknesses are now discussed in the paper according to the above-mentioned structure.

17. Figure 2: A and B: What do the error bars denote: standard error or standard mean? Please specify in the legends; C: Please include a scale bar for the image; E: What does T2WI stand for? Please mention in the figure legend.

Thank you for this helpful comment. In Figure 2A and 2B, the error bars denote the SEM, and this was specified now in the figure legends. We also added a scale bar to Figure 2C. “T2WI”st ands for T2 weighted image, and this was also clarified in the figure legends.

18. Figure 3: Please expand all abbreviations used in the figure in the figure legends.

All the abbreviations were expanded in the figure legend of Fig. 3.

Reviewer #1:

This manuscript covers an important topic related to the endovascular filament perforation model to mimic subarachnoid hemorrhage (SAH) - The strengths of the paper is that combined with magnetic resonance imaging (MRI) 24 hours after operation to ensure correct bleeding site, and the exclusion of other relevant intracranial pathologies. However, the paper could be substantially strengthened by addressing the following concerns.

We would like to thank reviewer #1 for the constructive comments, as well as careful and thorough consideration of our manuscript. We have addressed all the concerns and comments by reviewer #1. Below are our answers to the specific comments:

1. What is the reason of using ketamine/xylazine rather than isoflurane? Since ketamine has significant effect on the neuronal morphology and synaptic plasticity. How authors are sure about this issue?

Ketamin-Xylazin anesthesia is known to be effective against pain and distress, which makes it very suitable for this model. Although there is data in the literature showing an effect of neuronal morphology and synaptic plasticity, in our experimental groups we always carry out control

mice groups (Sham operation and baseline condition without surgery), and the quantified data on neuronal density, neuronal apoptosis and their association with microglia does show a significant impact that could be attributed to the surgery. We use isoflurane anesthesia as an alternative in imaging studies routinely. The ketamine/xylazine anaesthesia, however, has the advantage that it can be used anywhere, including operative rooms where inhalation anaesthesia is not available.

2. How ICP of mice during procedure was monitored?

We do not routinely monitor the ICP of mice in the procedure.

3. What is a reason of selecting MRI time point at 24 hours after surgery? While bleeding may accrue at earlier time point?

The postoperative MRI scans were taken 24 hours after the surgery to detect not only subarachnoid hemorrhage and possible hyperacute infarct demarcation but also subacute complications such as hydrocephalus and late infarct demarcation. We emphasized this in the updated version of the manuscript now.

4. How was the sex of mice in this experiment? how many male and female? Age of the mice? Wight?

All the mice be used in the studies are male and the age are 8-12 weeks. The weight was at 25±0.286 g (average +/-s.e.m.).

5. It is important to mention detail of mortality within 48 hours which means that how many at first 6 hours, then it make is easier to correlate this finding with the time point of MRI

Thank you for the point made here. We refined the manuscript accordingly.

6. Why only 50 mice went under MRI out of 92 mice?

As 12 out of 92 mice died during the first 48 postoperative hours, not all of them could be included in the MRI analyses. Moreover, a total number of 30 mice was examined via MRI at earlier time points to elicit the time dependence to acquire the best depiction of both SAH and early complications that come along with the surgery.

7. Which ANOVA test was used for the statistical analysis?

For the statistical analysis of SAH bleeding grade, the nonparametric one-way ANOVA was used as we made comparisons between multiple groups. This aspect was also added to the manuscript.

8. How the normal distribution of data was examined?

The normal distribution of data was examined with the Shapiro Wilk test.

9. How the variation within each group was examined?

We analyzed the variation with the Brown-Forsythe test, since the Shapiro Wilk test showed that the data are not Gaussian distribution.

10. Which variables were tested by using ANOVA?

Since the bleeding grade is defined by the volume and thickness in the clinical setting of SAH patients, we only analyzed for one variable which is the bleeding area defined by T2 weighted MRI imaging.

11. There are 4 grades of SAH , however in the plots only 3 grades are presented?

Analogous to the radiological grades in the literature for aneurysmal SAH patients, in which the bleeding grades ranges between no blood and a range of thickness of SAH blood in imaging studies, we defined grade 0 as “no bleeding” in the MRI. Grade 4 was considered as intracerebral hemorrhage which is characterized and is defined as an exclusion criteria for subsequent analyses referring to SAH pathophysiology. For the sake of completeness, please find below a figure with the bleeding volumes of grade 0-IV:

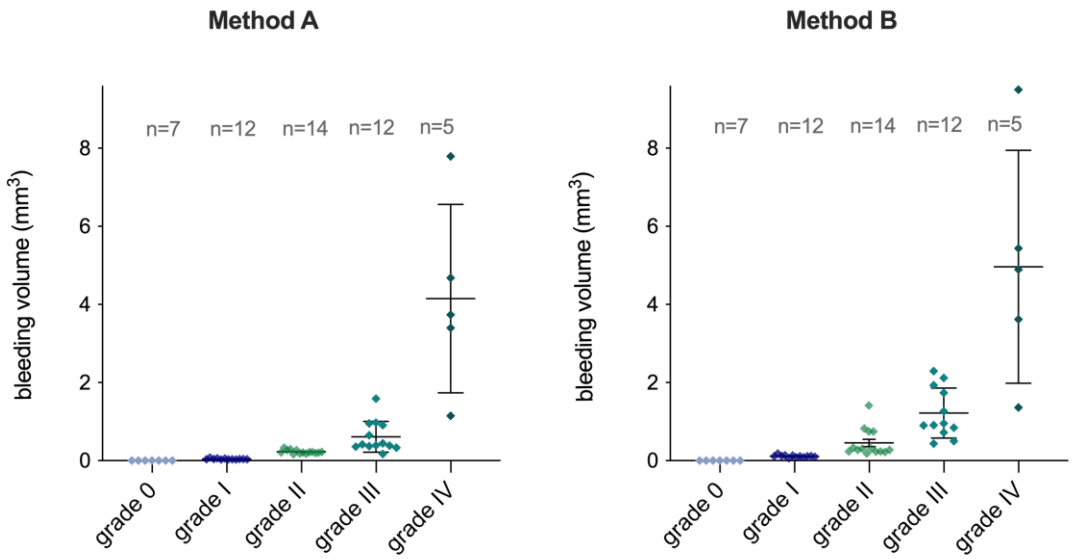

12. The grading system for bleeding is based on the anatomical level which means that at the level of ventral hippocampus is grade 4, so it is not the accurate grading, it should be comparison between the animals by the get the sum of the size of bleeding volume at all levels rather than grading.

Thank you for the point made here. We have now also included the quantification of grade 0 and grade IV in Fig. 2. We would like to clarify here that the radiological SAH grades in clinical practice are also based on the slice thickness on imaging studies such as the BNI score and the Fisher score. These SAH grades also correlate with the clinical outcome of SAH patients. Hence, we also aimed at creating a radiological score which graded the operatively induced SAH in their severity and is based on blood clot thickness. The blood volume here was a confirmation that the grades different significantly in bleeding area and were not just arbitrary. We changed the flow and order in the representative results section of the manuscript to strengthen this aspect.

13. There is no information of histological analysis of brain injury such as MAP2 staining to compare the results of MRI with histological findings as a gold standard.

As our study served to establish a method to grade subarachnoid hemorrhage severity based on MRI scans, we did not include intraparenchymal detection of brain injury markers in the first run. However, we agree with the reviewer entirely - additional histological stainings for brain injury markers are a useful complement to our presented study. We therefore added the notation that future studies will be combined with stainings of brain tissue and the subarachnoid space. As our study served to establish a method to grade subarachnoid hemorrhage severity based on MRI scans, we did not include intraparenchymal detection of brain injury markers in the first run.

Reviewer #2:

In this protocol, Dr. Liu and colleague provide the detail in establishing classical endovascular perforation subarachnoid hemorrhage model and verified by using 7T MRI scan. Generally, the protocol is well written, but a few concerns should be addressed before shooting the video.

We would like to thank reviewer #2 for the thoughtful and helpful comments and careful consideration of this manuscript. Please find below our point-by-point answers to the questions and comments.

1. In the animal preparation, what is the targeted temperature for "maintain normal body temperature", and for how long? Usually, we keep the mice warm until resuscitation.

The targeted body temperature during the operation ranges between 36,5 – 38 °C and the animals will be kept at least 2 hours postoperatively in a warming cage.

2. In SAH induction, how to prepare the filament? A slightly sharp tip would be helpful for the penetration.

Thanks for the important note here. We added to the manuscript that a slightly beveled tip is advantageous for adequate penetration of the vessel.

3. In Discussion, it would be better if the authors could briefly introduce what to do if the filament fail to forward into cranial.

The discussion section now contains a section about the troubleshooting during filament advancing. Withdrawing of the filament to the arterial trifurcation and adjusting of the head‘s position can be helpful in this case.

4. In MRI scan, is there an algorithm for the blood clot calculation more conveniently for junior researchers?

Thanks for the important remark here. We added a supplemental figure (Suppl. Fig. 1) in which more steps and details are shown on quantifying blood calculation with the freeware ImageJ.

5. In SAH bleeding grade, what is the criteria to grade SAH thickness into these five classifications? And how did the authors maintain relatively consistent for the blood volume into subarachnoid space for following experiments?

In our study, grade 0 was considered as an event without any bleeding, and grade 4 was considered as intracerebral hemorrhage. We graded these into the five grades based on the following:

- In the clinical setting, there are numerous studies grading SAH radiologically into different grades (Fisher Score, modified Fisher score and BNI score) [1; 2; 3]. All these three grading systems defined the grades by increasing severity of blood collection with the first grade representing SAH without signs of bleeding.
- For SAH animal studies, there are reports in the literature by Guo et al. [4] and Shishido et al. [5], in which the grading is classified into minimum, moderate, and massive.
- Hence, similar to the human existing grading scale we also graded our SAH mice into these five categories – with grade I-III being relevant for future studies (similar to the above-mentioned animal studies with categories “minimum, moderate, and massive”.

A standardized operation technique, puncture depth and filament size are the main means to control the amount of bleeding. Larger filament and deeper puncture depth will make the amount of bleeding greater. However, when dissecting all bleeding volumes

Reviewer #3:

Reject

We would like to thank Reviewer #3 for the consideration of the manuscript and regret that there they did not offer any insights on how the manuscript could be improved substantially.

Reviewer #4:

Manuscript Summary:

This study presented a standardized model for experimental aneurysmal SAH by endovascular perforation, combined with MR imaging 24 hours after surgery to confirm and grade the bleeding and to exclude other relevant intracranial pathologies. And this study established an MRI grading system that enables investigation of the severity of bleeding in experimental SAH without animal sacrifice.

Major weakness:

This study is well written in detail of the SAH model. However, this model is commonly used for many years and the experiences shared in this manuscript (such as adequate positioning of mice, intraoperative nerve protection, appropriate filament puncture depth) are not original and lack novelty. These is no description of the trick to reduce the mortality. Even though MRI is a good way to investigate the severity of bleeding, it is not easily available by most of the labs. The neurological score is a good way to evaluate the severity.

We would like to thank reviewer #4 for their careful consideration of the manuscript and the valuable critique. We absolutely agree with the reviewer that MRI might not always be available in research laboratories and might not always be a feasible method to investigate the severity of the bleeding. The neurological score as well as other investigations regarding secondary brain damage including microglia accumulation, neuronal apoptosis etc. represent still valuable assays to evaluate the further course in operatively induced SAH. However, the MRI still in our eyes is a valuable opportunity to assess for bleeding severeity as well as exclude other pathologies. Based on our data, in which we observed a 10% risk of inducing additional stroke or intracerebral hemorrhage detected by MRI. These are important co-ocurring pathologies that should be excluded from further analyses in order to have clean experimental groups. We have revised the discussion section accordingly:

"…Hence, in an attempt to classify the bleeding severity noninvasively, we added MRI imaging as a follow-up examination to grade SAH radiographically. This also ensured detection of false positive SAH animals and exclusion of other pathologies such as stroke, ICH and/or hydrocephalus. Some studies proposed intracranial pressure (ICP), cerebral perfusion, and blood pressure monitoring as evidence of successful SAH induction which might be additional helpful tools[23]. Another possible way to grade the severity of SAH and potential intraparenchymal damage is to combine the clinical findings with histological stainings for cell death markers such as p53, TUNEL or caspase-3. (Lee et al, Detection of Apoptosis in the Central Nervous System). Despite the advantages of MRI grading, there is one major drawback of this approach regarding its feasibility: MRI is not as widely available to labs as other methods. This limits the broad introduction of MRI grading systems in experimental SAH. When available, however, MRI provides an excellent tool to verify and quantify SAH extent."

Literature:

[1] J.A. Frontera, J. Claassen, J.M. Schmidt, K.E. Wartenberg, R. Temes, E.S. Connolly, Jr., R.L. MacDonald, and S.A. Mayer, Prediction of symptomatic vasospasm after subarachnoid hemorrhage: the modified fisher scale. Neurosurgery 59 (2006) 21-7; discussion 21-7.

[2] C.M. Fisher, J.P. Kistler, and J.M. Davis, Relation of cerebral vasospasm to subarachnoid hemorrhage visualized by computerized tomographic scanning. Neurosurgery 6 (1980) 1-9.

[3] D.A. Wilson, P. Nakaji, A.A. Abla, T.D. Uschold, D.J. Fusco, M.E. Oppenlander, F.C. Albuquerque, C.G. McDougall, J.M. Zabramski, and R.F. Spetzler, A simple and quantitative method to predict symptomatic vasospasm after subarachnoid hemorrhage based on computed tomography: beyond the Fisher scale. Neurosurgery 71 (2012) 869-75.
[4] D. Guo, D.A. Wilkinson, B.G. Thompson, A.S. Pandey, R.F. Keep, G. Xi, and Y. Hua, MRI Characterization in the Acute Phase of Experimental Subarachnoid Hemorrhage. Transl Stroke Res 8 (2017) 234-243.
[5] H. Shishido, Y. Egashira, S. Okubo, H. Zhang, Y. Hua, R.F. Keep, and G. Xi, A magnetic resonance imaging grading system for subarachnoid hemorrhage severity in a rat model. J Neurosci Methods 243 (2015) 115-9.

Editorial comments:

1. Please note that the manuscript has been formatted to fit the journal standard. Please review.

Thank you. We have reviewed the manuscript. The changes in the manuscript are marked in red color for easier reviewing.

2. Is the SAH grading system previously reported or is the grading system in the manuscript modified from any established protocols? In that case, please cite the relevant references. Also, please cite the references mentioned in the rebuttal in the manuscript.

The SAH grading system is based on established human grading which we modified based on a pre-existing mouse grading. These references had already been added to the manuscript. We have elaborated more on such in the discussion section.

> J.A. Frontera, J. Claassen, J.M. Schmidt, K.E. Wartenberg, R. Temes, E.S. Connolly, Jr., R.L. MacDonald, and S.A. Mayer, Prediction of symptomatic vasospasm after subarachnoid hemorrhage: the modified fisher scale. Neurosurgery 59 (2006) 21-7; discussion 21-7.
> C.M. Fisher, J.P. Kistler, and J.M. Davis, Relation of cerebral vasospasm to subarachnoid hemorrhage visualized by computerized tomographic scanning. Neurosurgery 6 (1980) 1-9.
> D.A. Wilson, P. Nakaji, A.A. Abla, T.D. Uschold, D.J. Fusco, M.E. Oppenlander, F.C. Albuquerque, C.G. McDougall, J.M. Zabramski, and R.F. Spetzler, A simple and quantitative method to predict symptomatic vasospasm after subarachnoid hemorrhage based on computed tomography: beyond the Fisher scale. Neurosurgery 71 (2012) 869-75.
> H. Shishido, Y. Egashira, S. Okubo, H. Zhang, Y. Hua, R.F. Keep, and G. Xi, A magnetic resonance imaging grading system for subarachnoid hemorrhage severity in a rat model. J Neurosci Methods 243 (2015) 115-9.

3. Please include the figure from the rebuttal (Reviewer #1, Q11) as a supplemental figure and provide a title and brief description in the Figure and Table legends section.

The figure was added as a supplemental figure S2 with Figure and Table legends section in the manuscript.

4. Please include a title and brief description for the Supplementary figure (step-by-step details on quantification) in the Figure and Table legends section.

A title and brief description of the supplementary figure (Fig. S1) was also added to the manuscript:

"Supplemental Figure 1: A step-by-step guide for quantifying bleeding volume with ImageJ. *Import the images with ImageJ, and enter "Strg+I" to show the dimensional data. Then set the scale for the image. Identify all the images in which SAH can be seen. For method A, identify the slice with the biggest bleeding area and measure the craniocaudal length (=a) as well as the mediolateral length (=b) of the two orthogonal axes that span the ellipsoid SAH volume. The ventrodorsal dimension (=c) of the ellipsoid shape can be estimated based on the slice thickness and the number of slices on which SAH is seen[c=slice thickness*number of slices]. Calculate the volume based on the formula: V= abc/2. For method B, measure the bleeding areas on each slice separately and then calculate the volume based on the formula:* $V = (A_1 + A_2 + \cdots + A_x) \cdot d$*, by which d= slice thickness."*

Supplemental Fig. S1

Click here to access/download;Supplemental File (Figures, Permissions, etc.);Fig. S1_RX.pdf

1. Open ImageJ software:

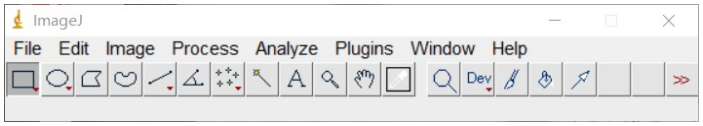

2. Import magnetic resonance sequence:

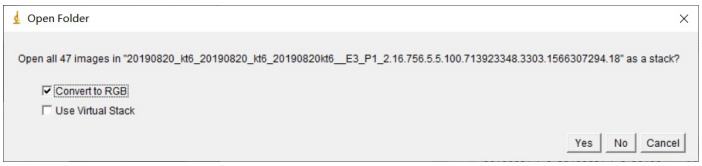

3. Enter „Strg+I“ to show info. Find dimensional data, e.g. slice thickness=0.35mm, width=25.6mm, height=25.6mm:

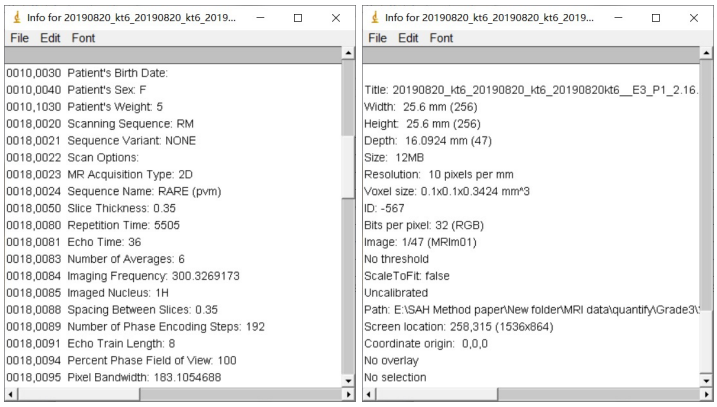

4. Set the scale based on the dimensional data or a scale bar (with which the image comes) by drawing a line on the known distance. Then go on „Analyze“→ „Set scale…“ and enter your specific values.

5. Identify all the images in which SAH can be seen (in these images T2 hypointense areas marked with *):

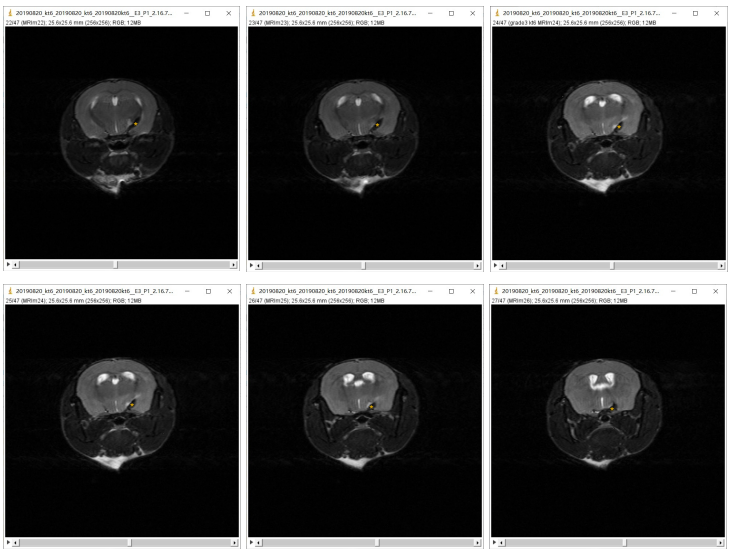

6. Method A: Identify the slice with the biggest bleeding area and measure the craniocaudal length *(=a)* as well as the mediolateral length *(=b)* of the two orthogonal axes that span the ellipsoid SAH volume.

The ventrodorsal dimension *(=c)* of the ellipsoid shape can be estimated based on the slice thickness [0.35mm] and the number of slices [6] on which SAH is seen.

Calculate the volume based on the formula:

V= abc/2.

*V= 2.24mm*0.637mm*(0.35mm*6)/2 = 1.498mm^3*

6. Method B: Select and alculate the bleeding areas separately:

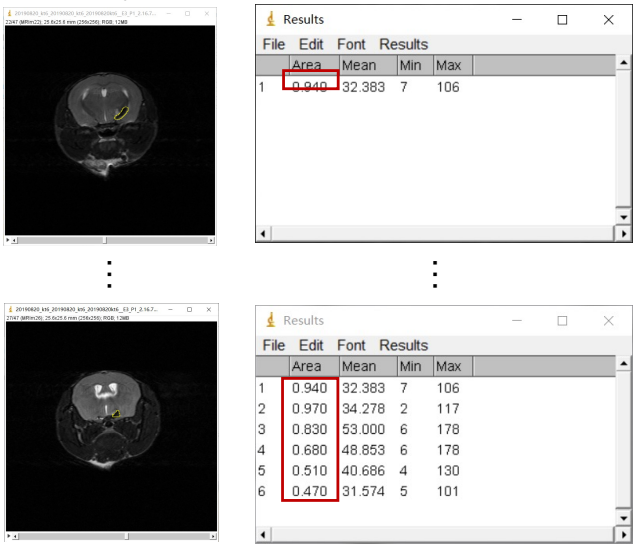

Calculate the volume based on the formula:

$V = (A_1 + A_2 + \cdots + A_x) \cdot d$
d= slice thickness

*V = (0.94mm^2+0.97mm^2+0.83mm^2+0.68mm^2+0.51mm^2+0.47mm^2) *0.35mm = 1.54 mm^3*

Supplemental Fig. S2

Click here to access/download;Supplemental File (Figures, Permissions, etc.);Fig. S2_RX.pdf

A

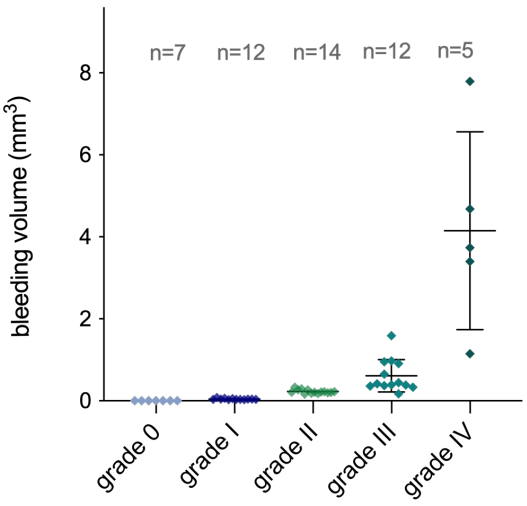

B